Research paper

Comprehensive survey of VUV induced dissociative photoionization of aniline: Role of H migration assisted isomerization

Muthuamirthambal Selvaraj [a], Arun Subramani [a], Karthick Ramanathan [a], Marco Cautero [b,c], Robert Richter [b], Nitish Pal [b], Paola Bolognesi [d], Lorenzo Avaldi [d], M.V. Vinitha [a], Chinmai Sai Jureddy [a], Umesh R. Kadhane [a,*]

[a] *Indian Institute of Space Science and Technology, Thiruvananthapuram, 695547, Kerala, India*
[b] *Elettra-Sincrotrone Trieste, Strada Statale 14 - km 163, 5 in AREA Science Park, Basovizza, TS 34149, Italy*
[c] *Dipartimento di Ingegneria e Architettura, University of Trieste, Trieste, 34127, Italy*
[d] *CNR-Istituto di Struttura della Materia, Area della Ricerca di Roma 1, Monterotondo, Roma, 00015, Italy*

HIGHLIGHTS

- Complete VUV dissociative photoionization profile of aniline fragmentation.
- Comprehensive computational survey of all the relevant decay channels.
- Role of H migration in isomerization and dissociation.
- First ever identification of HNCH and HCCN loss pathways from aniline.

GRAPHICAL ABSTRACT

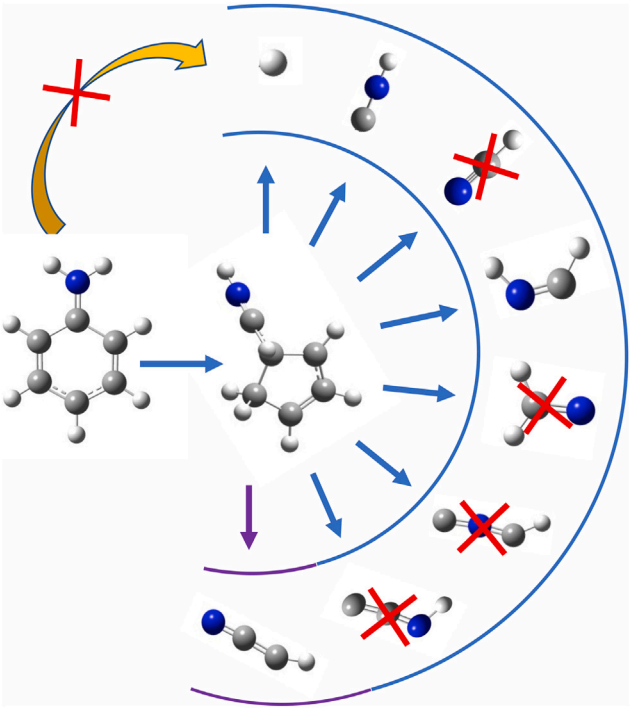

ARTICLE INFO

Keywords:
Aniline

ABSTRACT

A complete dissociation progression of aniline under VUV irradiation over the entire relevant internal energy range and inclusive of all decay channels is presented. The onset energy and breakdown curve was found

* Corresponding author.
E-mail address: umeshk@iist.ac.in (U.R. Kadhane).

VUV dissociative photoionization
H migration
Isomerization

to be instrumental in selecting relevant pathways out of multiple possibilities predicted by computation for all significant decay channels. The relevance of the ring contraction in the formation of the intermediate five-member ring structure and its consequences for the important channels such as HNC, H and HNCH losses are highlighted. In addition, a potential route for the formation of previously unexplored and astronomically important fragments HNCH and HCCN has been found. It could be deduced that aniline differs from its bicyclic nitrogenated counterpart, naphthalamine, as ring contraction in aniline is found to be favourable over ring expansion. Moreover, the role of H migration-assisted isomerization is highlighted in the context of the formation of astronomically important species.

1. Introduction

Five and six-membered monocyclic aromatics dominate terrestrial organic chemistry, widely serving as the building blocks of polymers and many biomolecules. Recent observations in Taurus molecular cloud (TMC-1) show the presence of nitrogenated monocyclic aromatics such as cyano benzene, 1-cyano-1,3-cyclopentadiene, and cyclopentadiene [1–3]. The observation of five-membered and six-membered rings in TMC-1 accentuates the relevance of nitrogenated aromatic chemistry in space [4,5]. Furthermore, numerous nitrogenated aromatics were found by the Cassini–Huygens mission on Titan, where high-energy radiation is known to drive chemical reactions. The nitrogenated smaller aromatics are expected to be crucial in the formation of larger polycyclic aromatic hydrocarbons (PAHs) and their nitrogenated counterparts (PANHs) in Titan and the interstellar medium (ISM) [6,7]. It is also possible that these nitrogenated aromatics are potential sources for other small nitrogen-containing molecules, like HNC, HCN, HCNH and HC_mN (where m> 1) in the ISM. For instance, the aforementioned small molecules have been observed in the collision-induced dissociation of amino-substituted PAHs ranging from naphthalene to pyrene [8], as well as the dissociative ionization of pyridine, benzonitrile and cyanonaphthalene [9,10]. These molecules are of great significance in understanding the astronomical environment; some are expected to lead to the formation of prebiotic molecules in those environmental conditions. Although they have been spread throughout various astronomical environments, it is challenging to replicate the sources of their densities using only conventional models, such as gas phase reactions. Therefore, it is essential to understand how these small molecules are produced either by a top-down or bottom-up approach. One of the important molecules; HNC has been discovered in significant quantities in a diversity of astrophysical environments, including diffuse interstellar clouds [11], prestellar discs [12,13], outflowing circumstellar envelopes [14,15], and planetary nebulae [16,17]. It is particularly prevalent in cometary comae [18–21] and the cores of cold, dense interstellar clouds in the ISM [11,22–28]. The increase in [HNC]/[HCN] ratio in comets with decreasing heliocentric distance corroborates the theory that the photodestruction of nitrogenated molecules may be the source of HNC abundance [14,29–31]. It is essential to comprehend the existence and synthesis of this molecule in such environments since HNC is closely linked to the formation and destruction of several other compounds, such as PANHs and their skeletons in ISM. Most of the nitrogenated mono and polycyclic aromatics have a common primary fragment due to mass 27 loss which corresponds to either HNC or HCN. It is challenging to experimentally identify the specific isomeric fragment in the photodissociation process.

Aniline, in particular, is an essential molecule to investigate the photodissociation mechanism which drives the molecular dynamics of nitrogenated aromatics in an interstellar environment. More specifically, it is known that aniline loses HNC exclusively as a fragment in the dissociative photoionization process. This is based on number of studies, including the time-resolved appearance energy of the HNC loss from aniline cation using trapped-ion mass spectrometry (TIPMS) [32]. The appearance energy of the mass 27 loss evaluated by Lifshitz et al. amply supports the thesis of HNC loss [32]. Density functional theory (DFT) has been used to study the structure and vibrational spectra of the singly charged aniline cation $C_6H_5NH_2^+$ [33] and to study the energetics of its dissociation leading to the loss of HNC and H fragments [34]. The isomerization preceding loss of HNC and H loss channels was discovered using electron impact ionization with isotopically labelled and deuterated aniline [35]. In addition, several studies on resonance-enhanced multiphoton dissociation of aniline have been conducted [36–40]. The fragmentation channels in the collision-induced dissociation of the protonated aniline molecular ion have also been studied and found to differ from those in the photoinduced dissociation method [41]. Intriguingly, HNC loss from aniline photodissociation as a primary channel is only detected in its ionic state and not in its neutral state [42]. The investigations based on the multimass imaging method has demonstrated that a significant portion of the neutral aniline's ground electronic state isomerizes and re-aromatizes to methylpyridine before dissociation [42]. This shows the fascinating behaviour of the atoms in the amino group being rearranged into the aromatic ring. Therefore, it is essential to comprehend how aniline dissociates and loses HNC as a function of internal energy and how this causes it to differ from its ground electronic state in both neutral and ionic nature.

Although there have been multiple investigations on aniline dissociations in the past, the subject still has a significant interest, as shown by recent results [43,44]. Despite various investigations, an in-depth study of the fragmentations over the relevant range of internal energy was never carried out. Moreover, the comparison of the branching ratios of all decay channels was not done. Most studies concentrated on the HNC or H loss channel, with little or no attention paid to the other channels. However, recent discoveries of protonated aniline [45] and the concurrent existence of HNC and HNCH in Titan's atmosphere have led us to look into the potential origins of these molecules via dissociative photoionization of aniline under vacuum ultraviolet (VUV) irradiation. Here a comprehensive and quantitative analysis of the dissociative photoionization of aniline under VUV irradiation was done at 23 eV photon energy using synchrotron radiation. The breakdown graph has been obtained to measure the onset energy of the different fragmentation channels and to assess the entire fragmentation process along with its branching ratios. All possible pathways were evaluated computationally, and those pathways which were found to have computed higher energy than the observed onset energy were disregarded. The possible structure and potential route for the astronomically significant fragment molecules corresponding to the masses 28 and 39 loss channel are proposed using the possible computed potential energy surfaces. The common intermediate for the major channels and the importance of the NH group rotation competing with the hydrogen migration to attain the intermediate is discussed. The primary decay channels and the possible permuted sequential decay channels have been discussed.

2. Experimental section

The experiment was carried out at the low-energy branch line of the GasPhase Photoemission beamline of the Elettra synchrotron (Trieste, Italy), using the velocity map imaging (VMI) time-of-flight (TOF) coincidence endstation. The performance of the beamline [46] and the spectrometer [47] have been described previously, so only a brief description of the experiment is provided here. As the beamline optics was optimized to cover the soft X-ray range, significant contamination of the radiation by higher-order light coming from the undulator

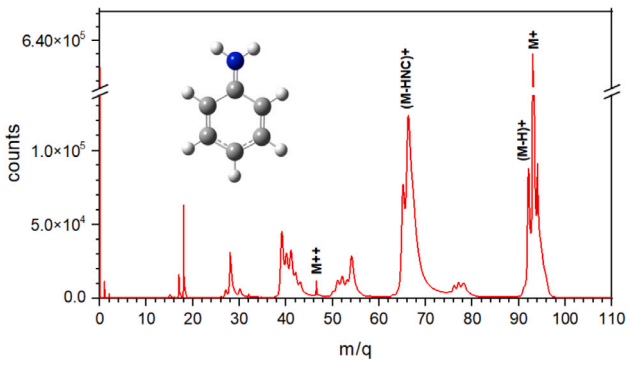

Fig. 1. Aniline mass spectrum recorded at 23 eV photon energy.

constitutes a problem at low energy. Therefore the branch line is equipped with a triply differentially pumped gas filter and a set of solid filters to cover different photon energy ranges. In the experiment described here, a 200 nm Sn foil filter [m/s Lebow Company] was used. A commercial liquid aniline sample was used without further purification. The vapour pressure of aniline is sufficiently high, so no heating was required for evaporation and the sample was used at room temperature. The target molecules were injected through a nozzle, and the effusive beam intersected with the photon beam in the source region of the spectrometer. The spectrometer can be operated in two separate modes. To measure the kinetic energy and angular distribution of the photoelectrons, the electrodes are biased to project the electrons onto the VMI side, equipped with a position sensitive crossed delay line detector, while the ions are sent towards the TOF (eVMI). By reversing the voltages applied to the electrodes, the instrument can also be used to measure the ions' kinetic energy distributions on the VMI side, collecting the (total) electrons on the TOF detector (iVMI). The measurement was performed in pulse-counting mode. The amplified and discriminated TOF signal was directed to an advanced 8-channel time-to-digital converter (TDC)[THR08-TDC], which is designed explicitly for coincidence measurements with delay line detectors. Meanwhile, the preamplified signals collected at the four ends of the detector itself were fed directly into the instrument's constant fraction discriminators. They were then used to compute the photoelectron impact coordinates (X, Y,t) directly on Intel's Cyclone 10 field-programmable-gate-array (FPGA) inside. The instrument's dual Gigabit Ethernet connections facilitated the real-time display of pre-processed coordinates while all raw timestamps were simultaneously saved for custom post-processing. The temporal precision of the instrument is adjustable down to 40 ps FWHM, although this can be traded off to increase the pulse-pair resolution. In this experiment, the configuration was set to a pulse-pair resolution of 12 ns and a temporal precision of 75 ps FWHM to capture data from as many ions as possible. The MEVELER algorithm [48] was used to extract the photoelectrons' angular and kinetic energy distribution from the corresponding image taken in the eVMI mode. The VMI spectrometer was calibrated in eVMI mode, recording Xe photoionization spectra at selected photon energies.

3. Computational details

Density functional theory calculations were performed using the GAUSSIAN 09 software [49]. Potential energy surface (PES) scans were performed at the B3LYP/6-311++ G(d,p) level of theory in order to locate the structures of the stationary points involved. The pathways with the lowest energy barrier leading up to each of the structures considered are reported. Geometries were optimized at the same level and vibrational frequencies were used to characterize the structures as minima (intermediates) and first-order saddle points (transition states). Intrinsic reaction coordinate (IRC) calculations were carried out for significant steps to verify that associate transition state indeed connects the local minima on either side.

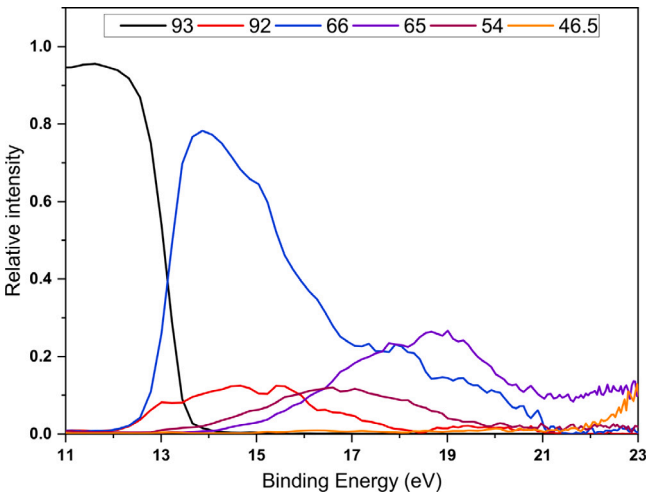

Fig. 2. Breakdown graph of the major dissociative channels of aniline. m/z 46.5 corresponds to the aniline dication.

4. Results and discussion

4.1. Time of flight mass spectra

The TOF mass spectrum of the aniline measured in iVMI mode at a photon energy of 23 eV is shown in Fig. 1. The intact parent molecular ion (m/z 93) $C_6H_7N^+$ showed the highest yield in the mass spectra. The m/z 66 is the most prominent aniline fragment, which has been shown in previous investigations to be HNC rather than HCN [32,38,50]. The next significant channels are m/z 92 and 65, corresponding to H and HNCH loss (or sequential loss of HNC and H), respectively. The m/z 54 peak corresponds to the possible loss of HCCN/HNCC/C_3H_3, which was not explored previously. The double ionization energy of aniline is 21.9 eV [51]; hence the dication peak has a reasonably modest intensity at the measured photon energy. Although the Sn filter was used in the beamline, it could only significantly reduce the higher-order harmonic photons rather than completely suppress them. As a result, the appearance of the dication in the mass spectrum may also be due to higher harmonics. Though the TOF resolution is reasonably good, other minor peaks are clustered around m/z 40–43 and m/z 50–53. Considering aniline being a small molecule with few fragment combinations, all ionic and neutral pairing possibilities have been explored for the observed peaks. For instance, the mass of the neutral moiety should be 42 if the charged detected fragment has a mass of m/z 51. It is possible to undergo HNC loss and then C_2H_2. Table 1 shows the observed ionic fragments and their neutral counterpart based on all possible permutations.

4.2. Breakdown curve and fragmentation progression

In Figs. 2 and 3, the yield of the coincidences between ions of selected m/z and photoelectrons with defined kinetic energy are reported versus the binding energy of aniline, i.e. the difference between the photon energy, 23 eV, and the kinetic energy of the photoelectrons. In the experiment, the set-up has been operated in the eVMI configuration. The relative intensity for each channel has been normalized to the sum of all channels observed in the mass spectrum to produce the breakdown curve. In Figs. 2 and 3, the sum of all ions does not add up to unity because the contribution of the aniline isotope (m/z 94) has not been included.

The appearance energy of the major channels and their relative yields are shown in Fig. 2. HNC and H loss channels were the first to be detected at 12 eV. HNC loss continues to dominate in the higher

Table 1
The various ionic fragments and their potential neutral counterparts.

No.	m/z	Ionic fragment	Neutral fragments	No.	m/z	Ionic fragment	Neutral fragments
1.	93	$C_6H_7N^{\cdot+}$		11.	51	$C_4H_3^{+}$	$NH_2 + C_2H_2$
2.	92	$C_6H_6N^{+}$	H	12.	50	$C_4H_2^{\cdot+}$	$NH_3 + C_2H_2$
3.	78	$C_6H_6^{\cdot+}$	NH			$C_4H_2^{+}$	$HNC + CH_4$
4.	77	$C_6H_5^{+}$	NH_2	13.	46.5	$C_6H_7N^{2+}$	
5.	76	$C_6H_4^{\cdot+}$	NH_3	14.	43	$C_2H_5N^{\cdot+}$	C_4H_2
6.	66	$C_5H_6^{\cdot+}$	HCN/HNC	15.	42	$C_3H_6^{\cdot+}$	HC_3N
7.	65	$C_5H_5^{+}$	HNCH/HNC+H	16.	41	$C_2H_3N^{\cdot+}$	$C_2H_2 + C_2H_2$
8.	54	$C_4H_6^{\cdot+}$	HCCN/HNCC	17.	40	$C_3H_4^{\cdot+}$	$C_2H_2 + HNC$
		$C_3H_4N^{+}$	C_3H_3			$C_3H_4^{+}$	$HNC + C_2H_2$
9.	53	$C_4H_5^{+}$	$H + HC_2N$	18.	39	HC_2N^{+}	$C_2H_2 + C_2H_4$
10.	52	$C_4H_4^{\cdot+}$	$NH + C_2H_2$	19.	28	CH_2N^{+}	$C_3H_3 + C_2H_2$

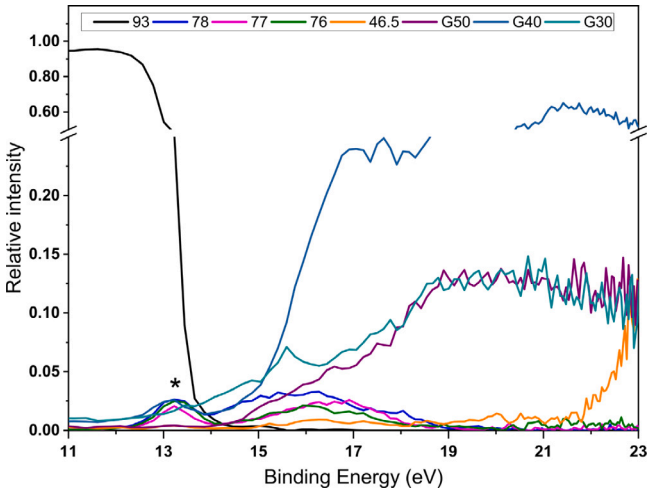

Fig. 3. Breakdown diagram of some of the minor channels of aniline. The slight jump in the yield indicated with the star is due to the contribution of the tail of m/z 66 to m/z 76–78.

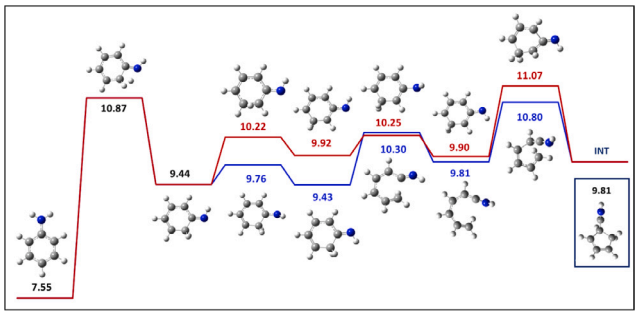

Fig. 4. Potential energy surface diagram for the five-membered ring intermediate structure (energy values in eV). The two pathways connected by the red and blue lines are described in the text.

energy region while the H loss channel decreases before HNC loss. The fragment corresponding to the mass 39 loss starts at around 14 eV and could be attributed to C_3H_3/HNCC/HCCN loss. The branching ratio of this channel is similar to the H loss channel. The yield of other minor channels has been plotted and shown in Fig. 3. Because it was difficult to distinguish the masses in the groupings around m/z 40 and 50 (except m/z 54), they were considered as a group and shown in a breakdown graph accordingly (indicated as G40 and G50). Since the m/z 66 channel undergoes metastable decay, the peak tail extends to m/z 78. Therefore, the minor structure between the 12 and 14 eV energy range is due to contamination from the m/z 66 channel, which adds to the m/z 76 to 78 decay channels.

4.2.1. HNC loss

Although m/z 66 could correspond to HCN loss, previous studies have conclusively assigned this mass 27 loss to HNC elimination [32, 50]. In addition, multiphoton ionization and electron impact ionization results agree with this assignment [35,36,38,40]. Therefore, we assume that the present observation of m/z 66 also exclusively corresponds to HNC loss.

Though the origin of HNC fragmentation has been explored computationally in several earlier studies, we revisit the calculations to present a complete picture and highlight a few interesting attributes. The HNC loss pathway described by Choe et al. [34] is implemented here to get the isomeric structure of an aniline cation with a five-membered ring (hereafter called INT), as shown in Fig. 4, which is a very important intermediate structure. The steps leading to this intermediate are shown in the figure. 4 with two possible mechanisms. In the previously reported pathway (blue line in Fig. 4), one hydrogen shifts from the amino group to the neighbouring carbon, causing the sp3 hybridization of that carbon. This is followed by cis-to-trans isomerization through the NH group reorientation, ring opening and closure to form INT structure. While this pathway is very plausible and has been reported before, a slightly different alternative is also considered here. It is proposed that a subsequent migration of the same H atom to the next carbon is possible before the reorientation of the NH group (red line in Fig. 4). This step may have a certain subtle impact on our understanding of how HNC and H loss occurs from aniline cation in general. This pathway does not involve the ring opening and closing while highlighting the importance of the dynamic transfer of the H atom from one carbon to the neighbouring carbon in competition with the NH reorientation. To elucidate the subtle implication of this competition, we use the experimental breakdown curve, which shows that the HNC and H loss channels appear together at 12 eV, indicating that these channels could come from similar stationary states or even the same intermediates. The calculated PES additionally showed a common INT structure between HNC and H loss channels. Even though the single H migration pathway occurs with lower energy than sequential H migration for the INT, sequential H migration brings the energy barrier between the HNC and the H loss routes closer as can be seen from Figs. 4 and 5. In any case, both pathways lead to INT, the most typical structure to lose HNC, where the final step is a loose transition with no reverse barrier.

To complete the discussion on the HNC loss channel, one can refer to the work by Baer and Carney [38], wherein it was found that m/z 66 is the cyclopentadiene cation (CP+), which is the same product found here computationally after the elimination of HNC (Fig. 5). Moreover, TIPMS experimental results [32] also confirms that the structure of the resultant molecular ion is CP+.

4.2.2. H loss

The H loss channel opens at 12 eV with the HNC loss channel and disappears at 18 eV, well before any other channel closes. The peak intensity of the H loss channel is approximately 12%, showing that the H loss is less favoured than the HNC loss in the fragmentation process. Computationally, the H loss pathway follows the same route as the HNC

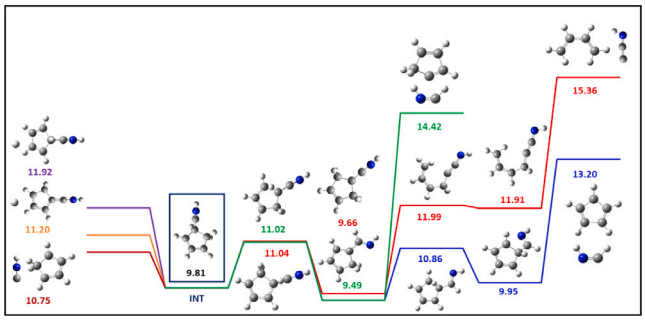

Fig. 5. Potential energy surface diagram (energy values in eV) for the loss of HNC and H (on the left side), HNCH and HNCC (on the right side) from the common intermediate five-membered structure.

loss till the INT structure. There are two potential routes for H loss from the intermediate INT. According to the theoretical study of Choe et al. [34], the sp3 carbon not carrying the C–N–H group may lose its hydrogen. Here we have proposed that the hydrogen loss occurs from the carbon-bearing C–N–H group, in agreement with Rap., et al. [43]. The proposed route (11.20 eV) here is less energetic than the alternate route (11.92 eV) [34]. Moreover, as mentioned in the previous section, this route is more likely because the energy barrier is close to the HNC loss route. In addition, the kinetic shift of the H loss channel is unknown, and the onset energy is approximately 12 eV; therefore, the lowest possible energy pathway could be assigned. This pathway leads to the formation of the 1H-cyanocyclopentadiene (cyano-CP+) product ion. The infrared spectroscopy results of trapped aniline ion suggest that the final product could be cyano-CP^+ [43]. Alternatively, H can be removed directly from the amino group, but this pathway is energetically more expensive than the other two fragmentation routes.

4.2.3. HNCH loss

The peak due to the mass 28 loss appears at about 13.7 eV in the breakdown curve. Interestingly, this channel has a higher overall yield than the H loss channel, at about 28%. The m/z 65 peak, which corresponds to a loss of mass 28, can be ascribed to sequential loss of HNC and H, or HNCH or C_2H_4. Among these three processes, the C_2H_4 elimination from the parent aniline ion was computationally attempted without success. An unusual rearrangement of hydrogens for this fragmentation channel is expected to be energetically or entropically expensive. On the other hand, HNCH can conceivably be lost from the parent ion by following steps similar to those for the other fragments discussed. Though the HNCH radical is often observed in space, the available formation mechanism cannot completely explain the presence of this molecule. As discussed here, let us suppose that aniline is producing this fragment in the dissociative photoionization process then aniline and aniline-like molecules could be the sources of these molecules, which would explain the origin of the HNCH that was found.

Since the HNC and H loss channels open at lower energy than this channel, it may imply that mass 28 may be a loss of HNC followed by H in a sequence. Attempts were made to look for breakdown curve correlations on a similar line as it had been demonstrated for quinoline photo dissociation recently to identify the sequence of such a pathway [52]. However, no correlation was found between H or HNC loss channels with mass 28 loss. Additionally, the computed energy of the product ion formation for the sequential loss of HNC and H is about 14.5 eV, which is higher than the observed onset energy. Hence the m/z 65 channel is assigned to the loss of HNCH and PES calculations were used to evaluate the possible fragmentation route to lose HNCH from the parent ion. As mentioned previously, the stationary points in the PES with a considerably higher energy barrier than the onset energy of this channel have been excluded. We obtained the low-energy HNCH loss pathway through the same five-membered ring intermediate INT shown in Fig. 5. Starting from the INT structure, hydrogen migration can occur from the ring carbon to the carbon holding the NH group. As shown in Fig. 5, the structural rearrangement through H migration before eliminating the HNCH decreases the energy required for this route. This highlights how hydrogen migration can reduce the energy cost for the specific pathway.

4.2.4. HCCN loss

The intensity of the m/z 54 channel is comparable to the H loss channel. The possible neutral counterpart to this channel, i.e. mass 39, needs some consideration. This fragmentation channel follows the HNC and H loss channels as the fourth major channel opening at 12.75 eV. It may correspond to loss of C_3H_3, HNCC, or HCCN. In the past, it was hypothesized without computational support that mass 39 could be C_3H_3 [36,41]. If the C_3H_3 is lost, the amino group is left outside the benzene ring, implying a drastic structural rearrangement for this channel. We explored the possible fragmentation route for losing C_3H_3 without success. Other possibilities are the loss of HNCC (iminovinylidene) or HCCN (cyanomethylene), radicals which play an important role in astrophysics. Before assigning the formation pathways of these species, it is useful to understand their significance in an astronomical context since these fragments were not considered in previous studies of aniline dissociation. The radical–radical chemical process is a possible route for the formation of adenine in interstellar space using HCCN as a precursor with NH_2CH [53,54]. Moreover, HCCN is the primary reaction product in the molecular beam experiment of excited nitrogen and acetylene [55], which represents the most probable initial stage in the production of nitriles in Titan's upper atmosphere. HCCN has also been observed in TMC-1 dark clouds and circumstellar envelopes [56,57].

As shown in Fig. 5, similar to the steps on the potential energy surface of the HNC and H loss channel, HNCC could be lost via INT. Throughout the stationary points for the final product, the final loose transition state is the step with the highest energy, about 7.8 eV above the ionization potential. Since the observed onset energy of this channel is less than the computed energy required for this fragment route, HNCC loss can be discarded as the source of m/z 54. Instead of C_3H_3 or HNCC, HCCN loss may be the most feasible fragment, considering the structural stability of the fragment, energy barrier and minimal rearrangement required. Unlike other channels such as HNC, H and HNCH loss, the loss of HCCN follows a different route that does not involve the ring contraction to form INT structure. As depicted in Fig. 6, HCCN can detach from the parent ion in two ways. One in which the NH rotation competes with the H transfer, leading to the ring expansion and formation of the less stable intermediate seven-membered ring. In the other one the NH rotation is absent and only H migration occurs before the loss of the HCCN fragment. The H migration is intriguingly essential for fragmentation in both routes. Moreover, these suggested pathways lead to the final common intermediate, whereas the HCCN is lost by direct bond cleavage without a reverse activation barrier. Since there have been various attempts, but no success, to identify another low energy route for mass 39 loss. As a result, HCCN loss may be a reasonable choice for the m/z 54 channel in comparison to the other two possible fragments.

4.2.5. NH, NH_2 and NH_3 loss

Though the intensities of the NH_m(m=1,2,3) loss channels are low, the investigation of these channels is essential. For the loss of the NH fragment, the hydrogen must be transferred from the amino group to either a neighbouring carbon atom in the benzene ring or the carbon that holds the amino group, followed by stretching the C–N bond until it breaks. It is understood that the migration of the H atom from the NH2 group leads to weakening of C–N bond and hence direct cleavage of the C–N bond leading to NH_2 loss is expected to be unfavourable compared to NH loss. Observations supporting this understanding have already been made with multiphoton-induced dissociative ionization of

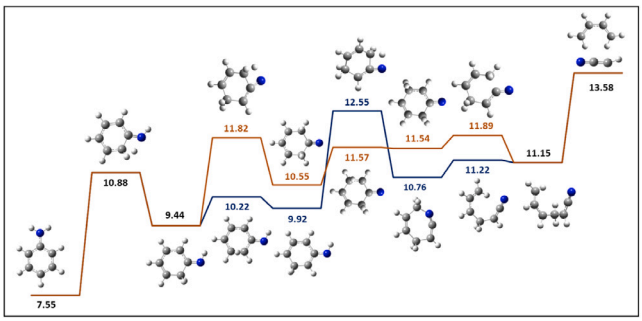

Fig. 6. Possible Potential energy diagram for HCCN loss channel (energy values in eV).

aniline [58]. On the contrary, the present measurements show loss of NH_2 neutral fragment with slightly lower but comparable propensity as NH loss. Therefore we consider that NH_2 is directly lost from the parent structure due to bond cleavage, which may be the plausible pathway for NH_2 loss as the structure is unaltered. Similarly, we observe the loss of NH_3, which is absent in the multiphoton experiment. To lose NH_3, hydrogen from the ring carbons must be transferred to the amino group, and *N* will undergo sp3 hybridization. This process can occur via H migration through the carbon atom or direct transfer to the nitrogen atom. Then the direct dissociation of the C–N bond will cause NH_3 to dissociate from the molecular ion.

It may be noted that the multiphoton experiment being referred to here was performed at 177.3 nm (7.0 eV), and only NH loss channel was observed. The difference in the observations by these two techniques can be understood in terms of the energetic. The total energy supplied to the target by the two-photon process was 14 eV, and only the NH loss channel was observed in the multiphoton work referred to here. On the other hand the present data shows no detectable intensity of NH_m(m=1,2,3) loss channels at 14 eV photon energy. All three channels appear at 15 eV photon energy, with the intensity of NH loss being substantially more than NH_2 or NH_3 loss channels. This asymmetry in the intensity NH_m (m=1,2,3) loss channels was observed to reduce as the photon energy was increased. Thus the difference in the observations made in the two experiments can be attributed to the higher internal energy, which makes the loss of NH_2 and NH_3 compete with the loss of NH.

4.2.6. C_2H_2 loss

While the loss of C_2H_2 is one of the prominent decay channels in all PAHs and, to a lesser extent, in PANHs, we observe a negligible amount of this decay in all the previously reported studies as well as present data. Attempts were made to compute such a pathway via all the possible intermediates without success. Hence it is concluded that C_2H_2 loss from the parent cation is not a viable channel over the entire energy range investigated here.

4.3. Sequential loss channels

As the peaks corresponding to the loss of mass 41, 42 and 43 cannot be separated in the recorded data, the branching ratios for these peaks are reported together, with their observed onset energy at 14 eV. Mass 41, 42 and 43 loss could result from the sequential loss of NH_m(m=1,2,3), followed by C_2H_2. The loss of mass 52 may result from the consecutive loss of two C_2H_2 and the formation of the $H_3C_2N^+$. Similarly, mass 53 loss could result from the consecutive loss of HNC and C_2H_2 to produce the propyne or allene ion $H_4C_3^+$. It is difficult to determine which fragment molecule may be responsible for the first loss in the sequential loss of the product fragments. The improbable nature of C_2H_2 loss being the first decay cahnnel implies that these sequential losses correspond to a first loss of the HNC or NH group followed by C_2H_2 loss. Fig. 7 shows the hierarchy of the sequential loss channel, combining the results from previous studies [36] and the ones of this work.

5. Implications of combining experimental and computational findings

Identifying specific dissociation pathways and the isomeric structure of the fragments is often a very complicated task requiring very detailed complex experimental and computational analysis. One of such methods consists in trapping the ion and identifying the fragment ions' structure by vibrational spectroscopy compared with the computed results [43,44]. By this technique, the structure of the fragment can be identified only after storing the fragment ion for a considerable amount of time. Since the fragment ion always has considerable internal energy and may undergo isomerization, the result may not represent the original fragment ion structure.

It has been observed that in the unimolecular dissociation of several cyclic aromatics, a straightforward bond cleavage is typically unfavourable. For example, even though hydrogen can be lost from the amino group through direct bond cleavage in aniline, it requires more energy than H loss after structural rearrangement. The result of deuterated aniline under electron impact ionization [35] also suggested that fragmentation channels, including the H loss channel, occur through structural rearrangements. The direct identification of the fragmentation route with or without isomerization is practically impossible in TOF mass spectra. Consequently, the onset energy obtained from the breakdown diagram and the energy of the computed pathways can be compared, allowing for the interpretation of possible stationary points in the PES. In the present work, stationary points with energies lower than the observed onset energy of the corresponding channels have been proposed as a viable alternative to stationary points with greater energies. Therefore, the combination of the experimental breakdown curves and computational results allows identifying specific isomers of fragments as well as specific pathways for the same isomer.

6. Conclusion

The statistical decay spectrum of nitrogenated aromatics is more diverse than pure carbon-hydrogen-based aromatics due to numerous additional neutral loss channels like HCN/HNC, HCNH/H_2CN, HCCN/HNCC etc. These product fragments are significant due to their abundant presence in several astronomical environments. The recent discoveries of large quantities and a large variety of nitrogenated aromatics in the members of our solar system, as well as interstellar medium, suggest that dissociative photoionization of the observed nitrogenated species of aromatics may inject or govern the abundance of the neutral fragments mentioned above. Hence, understanding these dissociative processes has become very important in recent years. Unlike pure PAHs, the nitrogen-containing fragments have more diversity of isomeric structures. The ratios of such isomers can become proxies to study the specific astronomical and astrochemical surroundings. One of the best examples in astronomical research is represented by the HNC and HCN ratio.

The present work finds that even the smallest nitrogenated aromatics, aniline, opens possibilities to produce at least three astronomically crucial fragments (such as HNC, HNCH and HCCN) and their isomers. This work not only elucidates their origin and energy dependence from the parent aniline cation but also presents an elaborate process of structural alterations before the dissociation. An attempt is made to understand these changes since their fundamental quantum chemistry could be common to the whole family of nitrogenated aromatics, especially during VUV-induced dissociative photoionization.

In summary, a complete VUV PEPICO measurement was performed on the aniline molecule, and the overall dissociation products were investigated. HNC and H loss are two channels that open earlier than others at 12 eV. The loss of HNC transforms into a cyclopentadiene fragment ion. Similarly, 1-cyano-CP ion is the end-product of H loss. These two product structures have already been found experimentally, and the present PEPICO findings and calculations corroborate the same

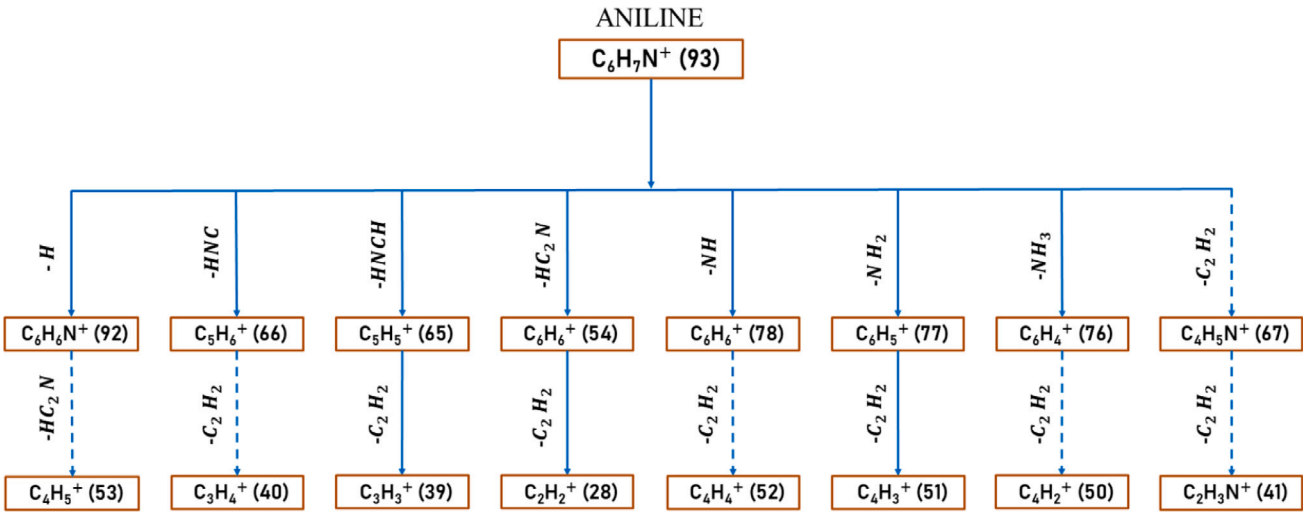

Fig. 7. Estimated hierarchy of the decay pathways for each mass. The major decay channels are represented by solid arrows, while possible permuted sequential loss channels are indicated by dotted arrows. Since the peaks due to C_2H_2 and HNC loss are overlapping in the mass spectrum, the C_2H_2 loss channel is represented by dotted arrow.

conclusion. The mass 39 loss fragment might be a neutral HNCC, HCCN, or C_3H_3 loss. Using the computed PES, we identified that the most plausible product amongst these fragments is the loss of HCCN, one of the astronomically significant species. The magnitude of NH_m(m=1,2,3) loss channels may be small, but they show how crucial hydrogen migration is in producing these decay channels. Though isomerizing to a seven-member ring is energetically equivalent to the pathway for losing HNC and H, aniline molecular ion prefers to proceed in the path of ring contraction, as evidenced by the prevalence of HNC and H loss. In addition, the HNC and H loss channels share common onset energy, which strongly indicates that both channels originate from the same isomeric structure. The aniline isomer, methyl pyridine, undergoes a seven-membered ring isomerization, dissociates, and re-aromatizes, much like toluene. Similarly, most PAH and their nitrogen equivalents (PANHs) prefer to form a seven-member ring before dissociating. However, aniline prefers to shrink the ring to a five-membered structure, which differs from its aromatic family. At the same time, the two approaches in isomerization produce an identical set of neutral fragments. The complete implications of this trend in aniline will be further explored by comparing it with a few more example molecules in future.

CRediT authorship contribution statement

Muthuamirthambal Selvaraj: Conceptualization, Methodology, Formal analysis, Data curation, Writing – original draft, Visualization, Investigation. **Arun Subramani:** Conceptualization, Writing – review & editing. **Karthick Ramanathan:** Conceptualization, Writing – review & editing. **Marco Cautero:** Resources, Software. **Robert Richter:** Resources, Conceptualization, Writing – review & editing. **Nitish Pal:** Resources. **Paola Bolognesi:** Resources, Conceptualization, Writing – review & editing. **Lorenzo Avaldi:** Resources, Conceptualization, Writing – review & editing, Funding acquisition. **M.V. Vinitha:** Conceptualization, Writing – review & editing. **Chinmai Sai Jureddy:** Conceptualization, Writing – review & editing. **Umesh R. Kadhane:** Resources, Conceptualization, Investigation, Writing – review & editing, Supervision, Funding acquisition.

Declaration of competing interest

The authors declare that they have no known competing financial interests or personal relationships that could have appeared to influence the work reported in this paper.

Data availability

Data will be made available on request.

Acknowledgement

The authors acknowledge the support provided by the 2022–024 Indo-Italian programme for exchange of researchers “Genesis of organic molecules in the extra-terrestrial environment : role of energetic radiation” and the funds provided by a grant from the Italian Ministry of Foreign Affairs and International Cooperation and the Indian Department of Science & Technology.

References

[1] A.M. Burkhardt, K.L.K. Lee, P.B. Changala, C.N. Shingledecker, I.R. Cooke, R.A. Loomis, H. Wei, S.B. Charnley, E. Herbst, M.C. McCarthy, et al., Discovery of the pure polycyclic aromatic hydrocarbon indene (c-C9H8) with GOTHAM observations of TMC-1, Astrophys. J. Lett. 913 (2) (2021) L18.

[2] J. Cernicharo, M. Agúndez, C. Cabezas, B. Tercero, N. Marcelino, J.R. Pardo, P. de Vicente, Pure hydrocarbon cycles in TMC-1: Discovery of ethynyl cyclopropenylidene, cyclopentadiene, and indene, Astron. Astrophys. 649 (2021) L15.

[3] B.A. McGuire, A.M. Burkhardt, S. Kalenskii, C.N. Shingledecker, A.J. Remijan, E. Herbst, M.C. McCarthy, Detection of the aromatic molecule benzonitrile (c-C6H5CN) in the interstellar medium, Science 359 (6372) (2018) 202–205.

[4] M.C. McCarthy, B.A. McGuire, Aromatics and cyclic molecules in molecular clouds: A new dimension of interstellar organic chemistry, J. Phys. Chem. A 125 (16) (2021) 3231–3243.

[5] A.M. Burkhardt, R.A. Loomis, C.N. Shingledecker, K.L.K. Lee, A.J. Remijan, M.C. McCarthy, B.A. McGuire, Ubiquitous aromatic carbon chemistry at the earliest stages of star formation, Nat. Astron. 5 (2) (2021) 181–187.

[6] D.S. Parker, R.I. Kaiser, On the formation of nitrogen-substituted polycyclic aromatic hydrocarbons (NPAHs) in circumstellar and interstellar environments, Chem. Soc. Rev. 46 (2) (2017) 452–463.

[7] R.I. Kaiser, D.S. Parker, A.M. Mebel, Reaction dynamics in astrochemistry: Low-temperature pathways to polycyclic aromatic hydrocarbons in the interstellar medium, Ann. Rev. Phys. Chem. 66 (2015) 43–67.

[8] J. Burner, B.J. West, P.M. Mayer, What will photo-processing of large, ionized amino-substituted polycyclic aromatic hydrocarbons produce in the interstellar medium? J. Phys. Chem. A 123 (24) (2019) 5027–5034.

[9] D.B. Rap, A. Simon, K. Steenbakkers, J.G. Schrauwen, B. Redlich, S. Brünken, Fingerprinting fragments of fragile interstellar molecules: Dissociation chemistry of pyridine and benzonitrile revealed by infrared spectroscopy and theory, Faraday Discuss. (2023).

[10] M.H. Stockett, J.N. Bull, H. Cederquist, S. Indrajith, M. Ji, J.E. Navarro Navarrete, H.T. Schmidt, H. Zettergren, B. Zhu, Efficient stabilization of cyanonaphthalene by fast radiative cooling and implications for the resilience of small PAHs in interstellar clouds, Nature Commun. 14 (1) (2023) 395.

[11] B. Turner, L. Pirogov, Y. Minh, The physics and chemistry of small translucent molecular clouds. VIII. HCN and HNC, Astrophys. J. 483 (1) (1997) 235.
[12] A. Dutrey, S. Guilloteau, M. Guelin, Chemistry of protosolar-like nebulae: The molecular content of the DM Tau and GG Tau disks, Astron. Astrophys. 317 (1997) L55–L58.
[13] E. Dartois, M. Gerin, L. d'Hendecourt, Multi-wavelength observations of the massive YSO RAFGL7009s, Astron. Astrophys. 361 (2000) 1095–1111.
[14] V. Bujarrabal, A. Fuente, A. Omont, Molecular observations of O-and C-rich circumstellar envelopes, Astron. Astrophys. 285 (1994) 247–271.
[15] S. Fukasaku, Y. Hirahara, A. Masuda, K. Kawaguchi, S.-I. Ishikawa, N. Kaifu, W.M. Irvine, Observations of molecular envelopes of late-type stars: CRL 618, CRL 2688, CRL 3068, and CIT 6, Astrophys. J. 437 (1994) 410–418.
[16] D. Schmidt, L. Ziurys, New detections of HNC in planetary nebulae: Evolution of the [HCN]/[HNC] ratio, Astrophys. J. 835 (1) (2017) 79.
[17] J. Bublitz, J.H. Kastner, M. Santander-García, V. Bujarrabal, J. Alcolea, R. Montez, A new radio molecular line survey of planetary nebulae-HNC/HCN as a diagnostic of ultraviolet irradiation, Astron. Astrophys. 625 (2019) A101.
[18] D. Lis, J. Keene, K. Young, T. Phillips, D. Bockelée-Morvan, J. Crovisier, P. Schilke, P. Goldsmith, E. Bergin, Spectroscopic observations of comet C/1996 B2 (Hyakutake) with the Caltech Submillimeter Observatory, Icarus 130 (2) (1997) 355–372.
[19] W.M. Irvine, E.A. Bergin, J.E. Dickens, D. Jewitt, A.J. Lovell, H.E. Matthews, F.P. Schloerb, M. Senay, Chemical processing in the coma as the source of cometary HNC, Nature 393 (6685) (1998) 547–550.
[20] T. Hirota, S. Yamamoto, K. Kawaguchi, A. Sakamoto, N. Ukita, Observations of HCN, HNC, and NH3 in comet Hale-Bopp, Astrophys. J. 520 (2) (1999) 895.
[21] L. Ziurys, C. Savage, M. Brewster, A. Apponi, T. Pesch, S. Wyckoff, Cyanide chemistry in comet Hale-Bopp (C/1995 O1), Astrophys. J. 527 (1) (1999) L67.
[22] A. Wootten, N. Evans, R. Snell, et al., Molecular abundance variations in interstellar clouds, Astrophys. J. 225 (1978) L143–L148.
[23] P.F. Goldsmith, W.D. Langer, J. Ellder, E. Kollberg, W. Irvine, Determination of the HNC to HCN abundance ratio in giant molecular clouds, Astrophys. J. 249 (Part 1) (1981) 524–531.
[24] P.F. Goldsmith, W.M. Irvine, A. Hjalmarson, J. Ellder, Variations in the HCN/HNC abundance ratio in the Orion molecular cloud, Astrophys. J. 310 (1986) 383–391.
[25] W.M. Irvine, F.P. Schloerb, Cyanide and isocyanide abundances in the cold, dark cloud TMC-1, Astrophys. J. 282 (1984) 516–521.
[26] P. Pratap, J. Dickens, R.L. Snell, M. Miralles, E. Bergin, W.M. Irvine, F. Schloerb, A study of the physics and chemistry of TMC-1, Astrophys. J. 486 (2) (1997) 862.
[27] T. Hirota, S. Yamamoto, H. Mikami, M. Ohishi, Abundances of HCN and HNC in dark cloud cores, Astrophys. J. 503 (2) (1998) 717.
[28] E. Sarrasin, D.B. Abdallah, M. Wernli, A. Faure, J. Cernicharo, F. Lique, The rotational excitation of HCN and HNC by He: new insights on the HCN/HNC abundance ratio in molecular clouds, Mon. Not. R. Astron. Soc. 404 (1) (2010) 518–526.
[29] S. Rodgers, S. Charnley, On the origin of HNC in Comet Lee, Mon. Not. R. Astron. Soc. 323 (1) (2001) 84–92.
[30] W.M. Irvine, J. Dickens, A. Lovell, F. Schloerb, M. Senay, E. Bergin, D. Jewitt, H. Matthews, The HNC/HCN ratio in comets, Earth Moon Planet. 78 (1997) 29–35.
[31] S. Rodgers, S. Charnley, HNC and HCN in comets, Astrophys. J. 501 (2) (1998) L227.
[32] C. Lifshitz, P. Gotchiguian, R. Roller, Time-dependent mass spectra and breakdown graphs. The kinetic shift in aniline, Chem. Phys. Lett. 95 (2) (1983) 106–108.
[33] P.M. Wojciechowski, W. Zierkiewicz, D. Michalska, P. Hobza, Electronic structures, vibrational spectra, and revised assignment of aniline and its radical cation: Theoretical study, J. Chem. Phys. 118 (24) (2003) 10900–10911.
[34] J.C. Choe, N.R. Cheong, S.M. Park, Unimolecular dissociation of aniline molecular ion: A theoretical study, Int. J. Mass Spectrom. 279 (1) (2009) 25–31.
[35] A.V. Robertson, C. Djerassi, Mass spectrometry in structural and stereochemical problems. CLXV. study of skeletal rearrangements in carbon-13-labeled aromatic amines, J. Am. Chem. Soc. 90 (25) (1968) 6992–6996.
[36] H. Kühlewind, H. Neusser, E. Schlag, Multiphoton metastable ion spectra and ion dissociation kinetics: Analysis of the decay channels of the aniline cation with a reflectron time-of-flight instrument, J. Chem. Phys. 82 (12) (1985) 5452–5456.
[37] T. Dietz, M. Duncan, M. Liverman, R. Smalley, Efficient multiphoton ionization of jet-cooled aniline, Chem. Phys. Lett. 70 (2) (1980) 246–250.
[38] T. Baer, T.E. Carney, The dissociation dynamics of state selected metastable aniline ions by single and multiphoton ionization, J. Chem. Phys. 76 (3) (1982) 1304–1308.
[39] E.J. Bieske, A.S. Uichanco, M.W. Rainbird, A.E. Knight, Mass selected resonance enhanced multiphoton ionization spectroscopy of aniline–Ar n (n=3, 4, 5,...) van der Waals complexes, J. Chem. Phys. 94 (11) (1991) 7029–7037.
[40] L. Zandee, R. Bernstein, Laser ionization mass spectrometry: Extensive fragmentation via resonance-enhanced multiphoton ionization of a molecular benzene beam, J. Chem. Phys. 70 (5) (1979) 2574–2575.
[41] M.L. Quiniou, A.J. Yates, P.R. Langridge-Smith, Laser photo-induced dissociation using tandem time-of-flight mass spectrometry, Rapid Commun. Mass Spectrom. 14 (5) (2000) 361–367.
[42] C.-M. Tseng, Y.A. Dyakov, C.-L. Huang, A.M. Mebel, S.H. Lin, Y.T. Lee, C.-K. Ni, Photoisomerization and photodissociation of aniline and 4-methylpyridine, J. Am. Chem. Soc. 126 (28) (2004) 8760–8768.
[43] D.B. Rap, T.J. van Boxtel, B. Redlich, S. Brunken, Spectroscopic detection of cyano-cyclopentadiene ions as dissociation products upon ionization of aniline, J. Phys. Chem. A 126 (19) (2022) 2989–2997.
[44] D. Zeh, M. Bast, D.B. Rap, P.C. Schmid, S. Thorwirth, S. Bruenken, S. Schlemmer, M. Schaefer, Cryogenic messenger-IR ion spectroscopy study of phenol & aniline molecular ions and of the common fragment ion [C5H6]+ formed by EI-MS, J. Mol. Spectrosc. 378 (2021) 111453.
[45] A. Ali, E. Sittler Jr., D. Chornay, B. Rowe, C. Puzzarini, Organic chemistry in Titans upper atmosphere and its astrobiological consequences: I. Views towards cassini plasma spectrometer (CAPS) and ion neutral mass spectrometer (INMS) experiments in space, Planet. Space Sci. 109 (2015) 46–63.
[46] R. Blyth, R. Delaunay, M. Zitnik, J. Krempasky, R. Krempaska, J. Slezak, K. Prince, R. Richter, M. Vondracek, R. Camilloni, et al., The high resolution gas phase photoemission beamline, elettra, J. Electron Spectrosc. Relat. Phenom. 101 (1999) 959–964.
[47] P. O'keeffe, P. Bolognesi, M. Coreno, A. Moise, R. Richter, G. Cautero, L. Stebel, R. Sergo, L. Pravica, Y. Ovcharenko, et al., A photoelectron velocity map imaging spectrometer for experiments combining synchrotron and laser radiations, Rev. Sci. Instrum. 82 (3) (2011) 033109.
[48] B. Dick, Inverting ion images without abel inversion: maximum entropy reconstruction of velocity maps, Phys. Chem. Chem. Phys. 16 (2) (2014) 570–580.
[49] M.J. Frisch, G.W. Trucks, H.B. Schlegel, G.E. Scuseria, M.A. Robb, J.R. Cheeseman, G. Scalmani, V. Barone, B. Mennucci, G.A. Petersson, H. Nakatsuji, M. Caricato, X. Li, H.P. Hratchian, A.F. Izmaylov, J. Bloino, G. Zheng, J.L. Sonnenberg, M. Hada, M. Ehara, K. Toyota, R. Fukuda, J. Hasegawa, M. Ishida, T. Nakajima, Y. Honda, O. Kitao, H. Nakai, T. Vreven, J.A. Montgomery Jr., J.E. Peralta, F. Ogliaro, M. Bearpark, J.J. Heyd, E. Brothers, K.N. Kudin, V.N. Staroverov, R. Kobayashi, J. Normand, K. Raghavachari, A. Rendell, J.C. Burant, S.S. Iyengar, J. Tomasi, M. Cossi, N. Rega, J.M. Millam, M. Klene, J.E. Knox, J.B. Cross, V. Bakken, C. Adamo, J. Jaramillo, R. Gomperts, R.E. Stratmann, O. Yazyev, A.J. Austin, R. Cammi, C. Pomelli, J.W. Ochterski, R.L. Martin, K. Morokuma, V.G. Zakrzewski, G.A. Voth, P. Salvador, J.J. Dannenberg, S. Dapprich, A.D. Daniels, Farkas, J.B. Foresman, J.V. Ortiz, J. Cioslowski, D.J. Fox, Gaussian09 Revision E.01, Gaussian Inc., Wallingford CT, 2009.
[50] P.C. Burgers, J.L. Holmes, A.A. Mommers, J.K. Terlouw, Neutral products of ion fragmentations: HCN and HNC identified by collisionally induced dissociative ionization, Chem. Phys. Lett. 102 (1) (1983) 1–3.
[51] D. Ascenzi, J. Roithová, D. Schröder, E.-L. Zins, C. Alcaraz, Growth of doubly ionized C, H, N compounds in the presence of methane, J. Phys. Chem. A 113 (42) (2009) 11204–11210.
[52] U.R. Kadhane, M. Vinitha, K. Ramanathan, J. Bouwman, L. Avaldi, P. Bolognesi, R. Richter, Comprehensive survey of dissociative photoionization of quinoline by PEPICO experiments, J. Chem. Phys. 156 (24) (2022) 244304.
[53] V. Gupta, P. Tandon, P. Rawat, R. Singh, A. Singh, Quantum chemical study of a new reaction pathway for the adenine formation in the interstellar space, Astron. Astrophys. 528 (2011) A129.
[54] A. Misra, P. Tandon, Reaction between CH 2 and HCCN: A theoretical approach to acrylonitrile formation in the interstellar medium, Orig. Life Evol. Biospheres 44 (2014) 143–157.
[55] N. Balucani, M. Alagia, L. Cartechini, P. Casavecchia, G. Volpi, K. Sato, T. Takayanagi, Y. Kurosaki, Cyanomethylene formation from the reaction of excited nitrogen atoms with acetylene: a crossed beam and ab initio study, J. Am. Chem. Soc. 122 (18) (2000) 4443–4450.
[56] D. McGonagle, W.M. Irvine, A search for HCCN in molecular clouds, Astron. Astrophys. 310 (1996) 970–972.
[57] M. Guélin, J. Cernicharo, Astronomical detection of the HCCN radical-toward a new family of carbon-chain molecules? Astron. Astrophys. (ISSN: 0004-6361) 244 (1) (1991) L21–L24.
[58] L. Geng, H. Zhang, H. Wu, Z. Sun, Z. Luo, Ionization and dissociation of benzene and aniline under deep ultraviolet laser irradiation, Chin. J. Chem. Phys. 33 (5) (2020) 583–589.